https://doi.org/10.1016/j.scriptamat.2017.08.037

Highly stretchable kirigami metallic glass structures with ultra-small strain energy loss

S.H. Chen[1], K.C. Chan[1]*, T.M. Yue[1] and F. F. Wu[1,2]

[1]Advanced Manufacturing Technology Research Centre, Department of Industrial and Systems Engineering, The Hong Kong Polytechnic University, Hung Hom, Kowloon, Hong Kong.

[2]School of Materials Science and Engineering, Liaoning University of Technology, Jinzhou, 121001, China

* Corresponding author. Tel.: +852 27664981. E-mail address: kc.chan@polyu.edu.hk (K.C. Chan).

Abstract

Some highly stretchable kirigami metallic glass (MG) structures with ultra-small strain energy loss during cyclic loading are developed. Less than 3% of strain energy loss is achieved after 1000 loading/unloading cycles, which is much smaller than the Kapton or nanocompsoites-based kirigami structures. By optimizing the kirigami pattern design and smoothing the kirigami cuts may further reduce the stress energy loss, and one kirigami MG structure even shows no obvious strain energy loss. They are potentially useful for developing reversible mechanical metamaterials/devices or substrates of functional optoelectronic devices.

Key words: Metallic glasses; Kirigami structures; Elasticity; Strain energy loss; Cyclic loading.

Kirigami structures, based on the ancient art of paper cutting, are being used extensively to develop metamaterials with novel mechanical and functional properties [1-8]. They are potentially useful for developing optoelectronic and optical devices, such as stretchable lithium-ion batteries [9], solar cell tracking systems [3], beam steering devices [10,11], and triboelectric nanogenerators [12]. Besides the large apparent elasticity which can maintain the periodicity under cyclic loading, they have

programmable elasticity with accurately-engineered tilted angles and out-of-plane buckling orientation of the elements [3,13]. The kirigami approach can be used to obtain predictable strain-property relationships in mechanical metamaterials, which are beneficial for developing stretchable optoelectronic and mechanical metamaterials/devices [1]. For example, Lamoureux et al. have reported that kirigami-based stretchable solar cell trackers not only have increasing energy generation efficiency, without significantly increasing the installation costs, but also expand the application of solar tracking systems [3]. Xu et al. have developed beam steering devices using kirigami nanocomposites, which can serve as optical device components in radar systems [10]. However, to maintain a long serving life, it is required that kirigami structure-based devices can maintain their elastic performance after a large number of cyclic loadings, where conventional materials severely limit the cycle life and significantly hinder their applications [10]. It has been reported that the polyimide film kirigami structure has about 18% elastic strain energy loss after 1000 cycles [1], and Kapton kirigami solar trackers also have large elastic strain energy loss up to about 74% after 1000 cycles [3]. Therefore, there is a great need to reduce the strain energy loss of kirigami structures while maintaining the excellent elastic performance before more widespread applications of the kirigami structures in optoelectronic and mechanical metamaterials/devices can be achieved.

Metallic glasses (MGs), also known as amorphous metals, have high strength approaching the theoretical values and a relatively-larger elasticity of about 2% as compared with the conventional crystalline metals [14-16]. In this work, in order to improve the elastic performance of kirigami structures, we have developed some kirigami structures using MG films. The results have shown that kirigami MG structures not only possess programmable strechability similar to other material-based kirigami structures, but also have elasticity larger than 198% and ultra-small strain energy losses less than 3%. Kirigami MG structures could be used in mechanical metamaterials/devices or substrates for optoelectronic devices, opening a new window for developing kirigami structures with extended cycle life.

Four kinds of kirigami structures (two straight and two curved patterns) were fabricated using MG and stainless steel films, respectively, by photochemical machining (PCM) (Fig. 1). $Fe_{73.5}Si_{13.5}B_9Cu_1Nb_3$ MG films of thickness ~ 20 μm were fabricated by rapid quenching the liquid mixture of pure elements onto a high-speed roller under an Ar atmosphere. The amorphous state of the MG films was checked using standard X-ray diffraction (XRD) analysis on a Rigaku Smartlab X-ray diffractometer (see the XRD patterns in Fig. 1a inset). The 304 stainless steel films, with thickness of ~ 20 μm, were bought from the market. Details of the fabricating process of kirigami MG and stainless steel structures are given in Fig. 1a. Photo-resists were firstly spread on the surface of both kinds of films. Thereafter, exposure of the composite films to UV light creates varying kirigami patterns on the surface of the metal films. The patterned films were then immersed into corrosive solutions to remove the cuts in the films by etching. Finally, the kirigami MG structures and steel structures were prepared by removing the photo-resists. The kirigami structures were tested on an Instron 3344 materials testing machine with a load cell of ± 10 N. To characterize the elastic strain energy loss of the kirigami MG structures, 1000 cycles of loading/unloading were conducted. After the mechanical tests, the stress-concentration regions of the kirigami structures were inspected using SEM on a Jeol JSM-6490 scanning electron microscope. Finite Element Modelling (FEM) analysis of the buckling of the kirigami structures with pattern A has been conducted. The input material parameters for the MG films are 200 GPa for Young's modulus [17], 4000 MPa for yield strength [17] and 0.323 for the Poisson's ratio [18], respectively. The input material parameters for 304 stainless steel are 200 GPa for Young's modulus [19], 231 MPa for yield strength [19] and 0.28 for the Poisson's ratio [19], respectively.

Since a kirigami structure can evolve into a 3D structure during the loading process, the elasticity of the kirigami structure cannot be determined by the conventional elasticity rules from the linear stage of the stress-strain curves for rigid materials. In

order to determine the elastic strain of kirigami structures, cyclic loading was applied to stretch the kirigami structures by increasing the axial displacement step by step. The elasticity of the kirigami structures was determined by comparing the loading and unloading curves after each step in the loading/unloading process. The results have shown that kirigami stainless steel structures have elastic strains less than 62%, 59%, 28% and 57% for patterns A-D, respectively (Fig. 2), where the load decrease in the unloading curves, as compared with the loading curves, is obvious. While the kirigami MG structures have not shown an obvious decrease of load between the loading and unloading curves, suggesting elastic strains larger than 165%, 198%, 85% and 190% for patterns A-D, respectively. With increase of the dimensions of the kirigami patterns (d_1 and w_2 in Fig. 1b), the nominal elastic limits of the kirigami structures decrease significantly for both MG and stainless steel structures (Fig. 2a and 2c). On the other hand, by tuning the straight kirigami cuts into curved ones, the nominal elastic limits increase significantly for kirigami MG structures. In the case of kirigami stainless steel structures, significant increase in the elastic limit has not been observed, suggesting that the elastic performance of kirigami MG structures might be more sensitive to the change of the kirigami patterns.

The increase of the elasticity in the kirigami MG structures as compared with the kirigami stainless steel structures may result from the relatively high strength (4000 MPa for MG and 231 MPa for stainless steel) and the large elastic limit of the MGs, where the same orders of stress concentration on the kirigami structures can lead to plastic deformation in stainless steel while the MG is still in the elastic state [20]. The findings show that the elastic properties of the parent materials have significant impact on the elastic performance of kirigami metal structures, and the use of MG films as parent films could be an effective way to obtain large elastic strains for developing optoelectronic and mechanical metamaterials/devices. It should be noted that kirigami paper structures have an obvious change of the deformation regime from rigid elasticity to the out-of-plane buckling in the load-nominal strain curves [21], which is not observed in most kirigami MG/steel structures in the present work. This

is because that present MG and steel films have thicknesses of ~ 20 μm, which are far less than the distance between the cuts (d = 1 mm, 1.5 mm) [21].

Maintaining the periodicity of the kirigami structures with accurately-controlled mechanical and functional properties is an important aspect in achieving a long cycle life, which requires the kirigami structures to have negligible elastic strain energy loss. However, strain energy loss is unavoidable under cyclic loading for conventional materials, such as plastics and crystalline metals, where the fatigue life is limited, especially when stretched to plastic deformation. In this work, we show that the kirigami MG structures have ultra-small strain energy loss after 1000 cycles (due to the limited nominal elastic strains being less than 62%, the cyclic loading tests were not conducted for the kirigami stainless steel structures.). As shown in Fig. 3, at nominal strains reaching about 165%, 158%, 71% and 152% for patterns A-D, respectively, the load-nominal strain curves at cycle 1000 match well with the curves at cycle 1, implying small strain energy losses for 1000 cycles. By integrating the load-nominal strain curves, the strain energy loss of the kirigami MG structures with patterns A-C have been calculated as ~ 2.4%, ~ 2.8% and ~ 1.4%, respectively. No obvious strain energy loss was observed for kirigami MG structure with pattern D, where the curve at cycle 1000 almost duplicates the curve at cycle 1. The ultra-small strain energy loss is much smaller than the strain energy loss in the kirigami structures made of Kapton/GaAs [3] and nanocomposites [1].

Under applied loading, plastic deformation of the kirigami structures is initiated at the stress-concentration regions, as indicated by the dash circles in Fig. 4. It is known that the plastic deformation in MGs is highly localized in the thin layers of shear bands [22,23]. The stress-concentration regions of kirigami MG structures have been examined using scanning electron microscopy (SEM). It can be seen in Fig. 4, after 1000 cycles of loading, no shear band was observed, implying that the stress-concentration regions of the kirigami MG structures are still in the elastic state. This phenomenon agrees well with the ultra-small strain energy loss of the kirigami

MG structures after 1000 cycles of loading. For comparison, the stress-concentration regions of the kirigami MG structures at a nominal strain of about 230% were also examined using SEM (Fig. 4b), where a large number of shear bands can be observed, indicating the occurrence of plastic deformation at the stress-concentration regions beyond the elastic strain stage [24]. To give more insight into the deformation behavior in the stress-concentration regions of the kirigami structures, Finite Element Modelling (FEM) analysis of kirigami structures with pattern A has been conducted. At the onset of buckling of the elements, the stress-concentration regions of both the kirigami MG structures and stainless steel structures are in the elastic state (Fig. 4f). However, when the loading process proceeds, the stress-concentration regions of the kirigami MG structures can maintain the elastic state (Fig. 4g), while a large yield region at the stress-concentration regions of the kirigami stainless steel structure can be found. It can then be concluded that the relatively high strength and large elastic limit of MGs not only results in the large elastic strain of the kirigami structures, but also causes the kirigami structures to maintain an elastic state after 1000 loading/unloading cycles, enabling a longer cycle life. The observation of minute strain energy loss of the kirigami structures with patterns A-C may be due to that the outline of the cuts of the kirigami structures by PCM being insignificantly smooth where bulges could be observed in the SEM images (Fig. 4c), causing the formation of micro-stress-concentration sites [25]. Under cyclic loading, these micro-stress-concentration-sites may serve as origins for plastic deformation, leading to the elastic strain energy loss [26]. The fatigue of the stress-concentration regions of MGs under cyclic loadings may also contribute to the strain energy loss of the kirigami structures [27,28].

Kirigami structures have great potential for development as metamaterials/devices for mechanical and functional applications. Although the metal-based kirigami structures have the advantage of good combinations of high stiffness and strength, metal-based kirigami structures have rarely been reported. This might be due to limited elastic limit as compared with non-metals materials. In this work, we show that MGs with a

relatively high strength of 4000 MPa and a large elastic limit of 2% can be used to develop kirigami structures with large elastic strains. Combining the SEM observations and FEM analysis, we show that the increase of the elastic strain as compared with kirigami structures made of conventional stainless steel films results from the high strength and large elastic limit of MGs in which the stress-concentration region can still maintain an elastic state at a relatively large nominal strain. Even after 1000 loading/unloading cycles, the stress-concentration regions can still be maintained in the elastic state.

Moreover, with higher strength and larger elastic limit, kirigami MG structures show tunable stretchability by changing the kirigami patterns (Fig. 2), where the buckling of the elements is mainly controlled by the elastic deformation, even at large nominal strains reaching 198%. On the contrary, the elastic performance of the kirigami stainless steel structures has less dependence on the change of the kirigami patterns. Due to the relatively small strength and elastic limit of stainless steel, the buckling of the elements of the kirigami stainless steel structures can be easily affected by the plastic deformation at the stress-concentration regions even at small nominal strains less than 57%. Therefore, the present kirigami MG structures have a good combination of accurately-controlled stretchability, large elastic strain and ultra-small strain energy loss. By the optimizing the kirigami patterns or smoothing the cuts through optimizing the PCM process could further improve the elastic strain and reduce the strain energy loss of the kirigami MG structures. Kirigami MG structures have demonstrated great application potential for developing flexible structures and mechanical metamaterials/devices with reversible and reconfigurable structures, for example, beam steering devices in radar [10,11]. They can also be used to extend the cycle life of some functional metamaterials/devices by serving as substrates, such as in the solar tracking systems [3]. It should be pointed out that when the sample size decreases to nanoscale, the deformation mode and fracture behavior of MGs are changed [29,30], resulting in different deformation behavior of the Kirigami structures. For example, at submicron-scale, the increase of the elastic limit to about 5%

of MGs may further improve the stretchability of Kirigami MG structures [31]. Therefore, more efforts should be devoted to elucidate the size effect when using the Kirigami MG structures at varying scales, especially at submicron-scale or nanoscale. It is well known that the properties of architectured materials depend on the design of the topology, which can be stretching-dominated structures or bending-dominated structures [32,33]. In our work, the Kirigami MG structures are of ordered architecture, which are stretched from the initial rigid elastic regime to the out-of-plane buckling regime during the elastic deformation stage, leading to high stretchability. Such ordered structures are different from the disordered structures such as BMG foams which are bending-dominated.

In summary, highly stretchable kirigami MG structures have been developed, demonstrating ultra-samll elastic strain energy loss after 1000 loading/unloading cycles. The ultra-small strain energy loss is due to the relatively-high strength and large elastic limit of MGs. The stretchable kirigami MG structures may not only be used for developing mechanical metamaterials/devices, but can also be used as substrates to extend the cycle life of certain functional optoelectronic devices, expanding the practical structural-applications of MGs.

Acknowledgements

The work described in this paper was supported by a grant from the Research Committee of the Hong Kong Polytechnic University under research project No. 1-YW0R and a grant from the Faculty of Engineering of the Hong Kong Polytechnic University under research project No. 1-45-37-99QP.

References

[1] T.C. Shyu, P.F. Damasceno, P.M. Dodd, A. Lamoureux, L.Z. Xu, M. Shlian, M. Shtein, S.C. Glotzer, N.A. Kotov, Nat. Mater. 14 (2015) 785-789.

[2] M.K. Blees, A.W. Barnard, P.A. Rose, S.P. Roberts, K.L. McGill, P.Y. Huang,

A.R. Ruyack, J.W. Kevek, B. Kobrin, D.A. Muller, P.L. McEuen, Nature 524 (2015) 204-207.

[3] A. Lamoureux, K. Lee, M. Shlian, S.R. Forrest, M. Shtein, Nat. Commun. 6 (2015) 8092.

[4] B.G. Chen, B. Liu, A.A. Evans, J. Paulose, I. Cohen, V. Vitelli, C.D. Santangelo, Phys. Rev. Lett. 116 (2015) 135501.

[5] Y.H. Zhang, Z. Yan, K.W. Nan, D.Q. Xiao, Y.H. Liu, H.W. Luan, H.R. Fu, X.Z. Wang, Q.L. Yang, J.C. Wang, W. Ren, H.Z. Si, F. Liu, L.H. Yang, H.J. Li, J.T. Wang, X.L. Guo, H.Y. Luo, L. Wang, Y.G. Huang, J.A. Rogers, Proc. Natl. Acad. Sci. U.S.A. 112 (2015) 11757.

[6] F. Wang, X. Guo, J. Xu, Y. Zhang, C.Q. Chen, J. Appl. Mech. 84 (2017) 061007.

[7] S. Yang, I.S. Choi, R.D. Kamien, MRS Bull. 41 (2016) 130.

[8] M. Quisse, M. Collet, F. Scarpa, Smart Mater Struct 25 (2016) 115016.

[9] Z. Song, X. Wang, C. Lv, Y. An, M. Liang, T. Ma, D. He, Y.J. Zheng, S.Q. Huang, H. Yu, H. Jiang, Sci. Rep. 5 (2015) 10988.

[10] L. Xu, X. Wang, Y. Kim, T.C. Shyu, J. Lyu, N.A. Kotov, Acs Nano 10 (2016) 6156.

[11] W. Wang, C.Z. Li, H. Rodrigue, F.P. Yuan, M.W. Han, M. Cho, S.H. Ahn, Adv. Funct. Mater. 27 (2017) 1604214.

[12] C. Wu, X. Wang, L. Lin, H. Guo, Z.L. Wang, Acs Nano 10 (2016) 4652.

[13] Y. Tang, G. Lin, S. Yang, Y.K. Yi, R.D. Kamien, J. Yin, Adv. Mater. 29 (2017) 1604262.

[14] M.M. Trexler, N.N. Thadhani, Prog. Mater. Sci. 55 (2010) 759-839.

[15] A.R. Yavari, J.J. Lewandowski, J. Eckert, MRS Bull. 32 (2007) 635-638.

[16] W.H. Wang, Prog. Mater. Sci. 57 (2012) 487-656.

[17] K. Amiya, A. Urata, N. Nishiyama, A. Inoue, Mater. Trans. 45 (2004) 1214-1218.

[18] D.H. Kim, J.M. Park, G. Wang, R. Li, N. Mattern, J. Eckert, Appl. Phys. Lett. 96 (2010) 031905.

[19] T.R. Anthony, H.E. Cline, J. Appl. Phys. 49 (1978) 1248-1255.

[20] S.H. Chen, K.C. Chan, F.F. Wu, L. Xia, Sci. Rep. 5 (2015) 10302.

[21]M. Isobe, K. Okumura, Sci. Rep. 6 (2016) 24758.

[22]A.L. Greer, Y.Q. Cheng, E. Ma, Mater. Sci. Eng. R 74 (2013) 71-132.

[23]P.S. Steif, F. Spaepen, J.W. Hutchinson, Acta Metall. 30 (1982) 447-455.

[24]S.H. Chen, K.C. Chan, L. Xia, Intermetallics 43 (2013) 38-44.

[25]R.T. Qu, Q.S. Zhang, Z.F. Zhang, Scripta Mater. 68 (2013) 845-848.

[26]S.H. Chen, K.C. Chan, L. Xia, Mater. Sci. Eng. A 574 (2013) 262-265.

[27]G.Y. Wang, D.G. Harlow, P.K. Liaw, W.H. Peter, R.A. Buchanan, Acta Mater. 56 (2008) 3306-3311.

[28]J. Luo, K. Dahmen, P.K. Liaw, Y.F. Shi, Acta Mater. 87 (2015) 225-232.

[29]C.Q. Chen, Y.T. Pei, O. Kuzmin, Z.F. Zhang, E. Ma, J.T.M. De Hosson, Phys. Rev. B 83 (2011) 180201(R).

[30]D.T.A. Matthews, V. Ocelik, P.M. Bronsveld, J.T.M. De Hosson, Acta Mater. 56 (2008) 1762-1733.

[31]Q.S. Deng, Y.Q. Cheng, Y.H. Yue, L. Zhang, Z. Zhang, X.D. Han, E. Ma. Acta Mater. 59 (2011) 6511-6518.

[32]Y.H. Jiang, Q.M. Wang, Sci. Rep. 6 (2016) 34147.

[33]N.A. Fleck, V.S. Deshpande, M.F. Ashby, Proc. R. Soc. A 466 (2010) 2495-2516.

Figure 1

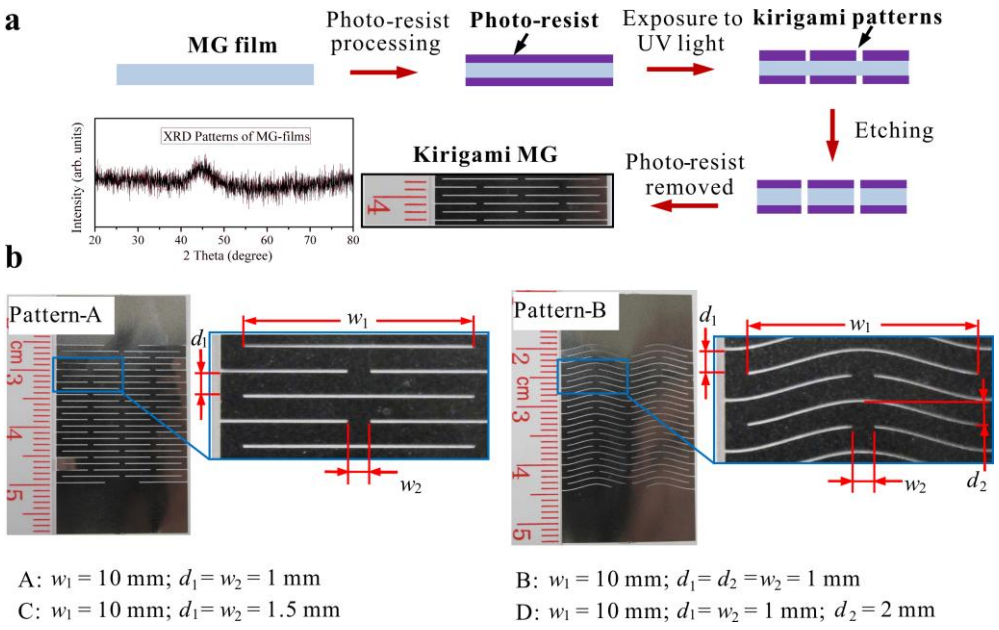

Figure 1. Fabrication of kirigami MG structures. (a) Fabrication process of kirigami MG structures using photochemical machining (PCM), where in inset XRD patterns confirm the amorphous state of the MG films; (b) Straight (A and C) and curved (B and D) patterns for fabricating kirigami MG structures, where the representative Patterns A and B are given as examples.

S.H. Chen *et al*.

Fig. 1

Figure 2

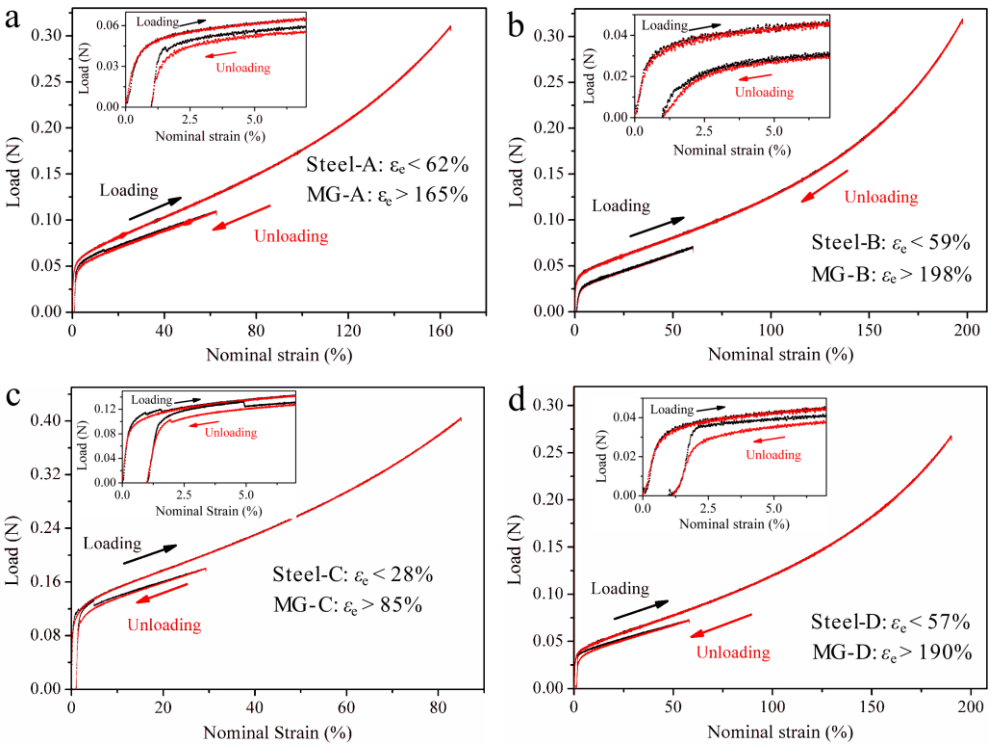

Figure 2. The elastic responses of the kirigami structures. The apparent elasticity of kirigami MG structures and kirigami stainless steel structures is obtained under cyclic loadings, where A-D denote the corresponding kirigami patterns in Figure 1, respectively, and ε_e is the nominal elastic strain limit.

S.H. Chen *et al.*

Fig. 2

Figure 3

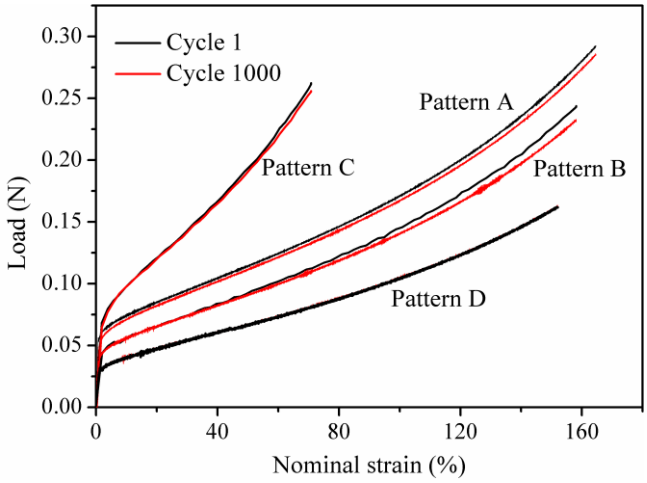

Figure 3. The elastic strain energy loss of kirigami MG structures. After 1000 cycles of loadings, the elastic strain energy loss for Patterns A-C are 2.4%, 2.8% and 1.4 %, respectively, and no obvious strain energy loss was observed in the specimens with pattern D.

S.H. Chen *et al.*

Fig. 3

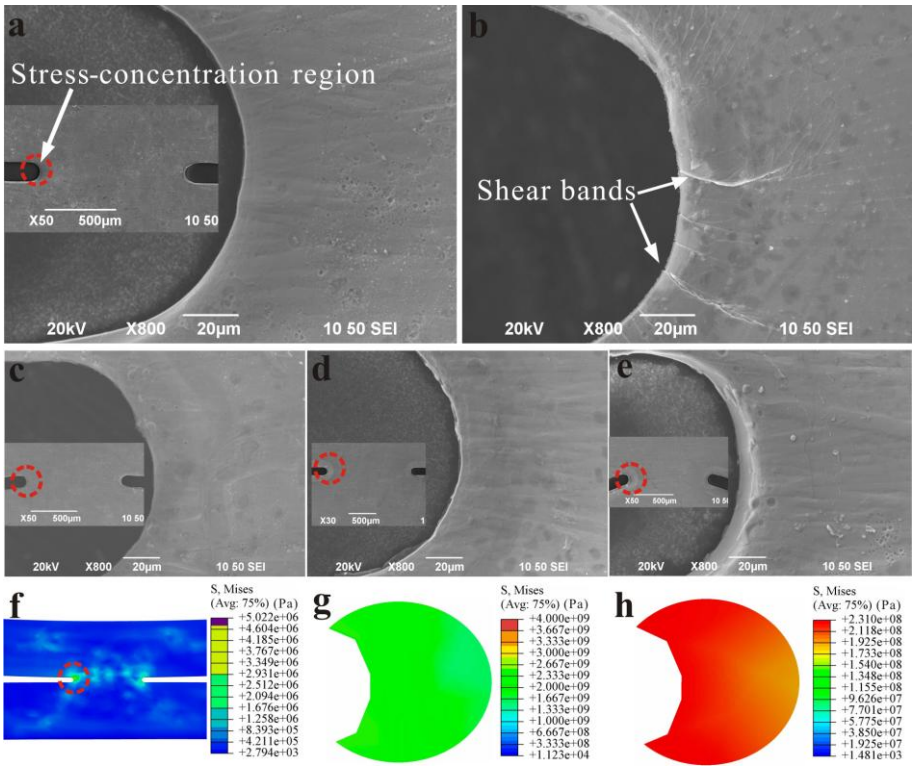

Figure 4. Deformation behavior of the stress-concentration regions (as indicated by the dash circles). (a and b) The SEM image of the stress-concentration regions of the kirigami MG structures (pattern A) with nominal strain of about 165% after 1000 cycles, where no shear band was observed (a). In contrast, the specimen at nominal strain of about 230% has shown a large number of shear bands (b), suggesting the occurrence of plastic deformation. (c-e) The SEM image of the stress-concentration regions of the kirigami MG structures for patterns B-D after 1000 cycles, where no shear band was observed, implying that these stress-concentration regions are still in an elastic state. (f-h) FEM results showing the stress distribution at the stress-concentration regions, where (f) is at the onset of buckling of the kirigami MG structure (the kirigami stainless steel structure has similar stress distributions), (g) is a magnified image of the stress-concentration region in (f) during the elastic stage, and (h) shows the yielding of the stress-concentration region of a kirigami stainless steel structure at the same nominal strain with (g).

***Graphical Abstract**

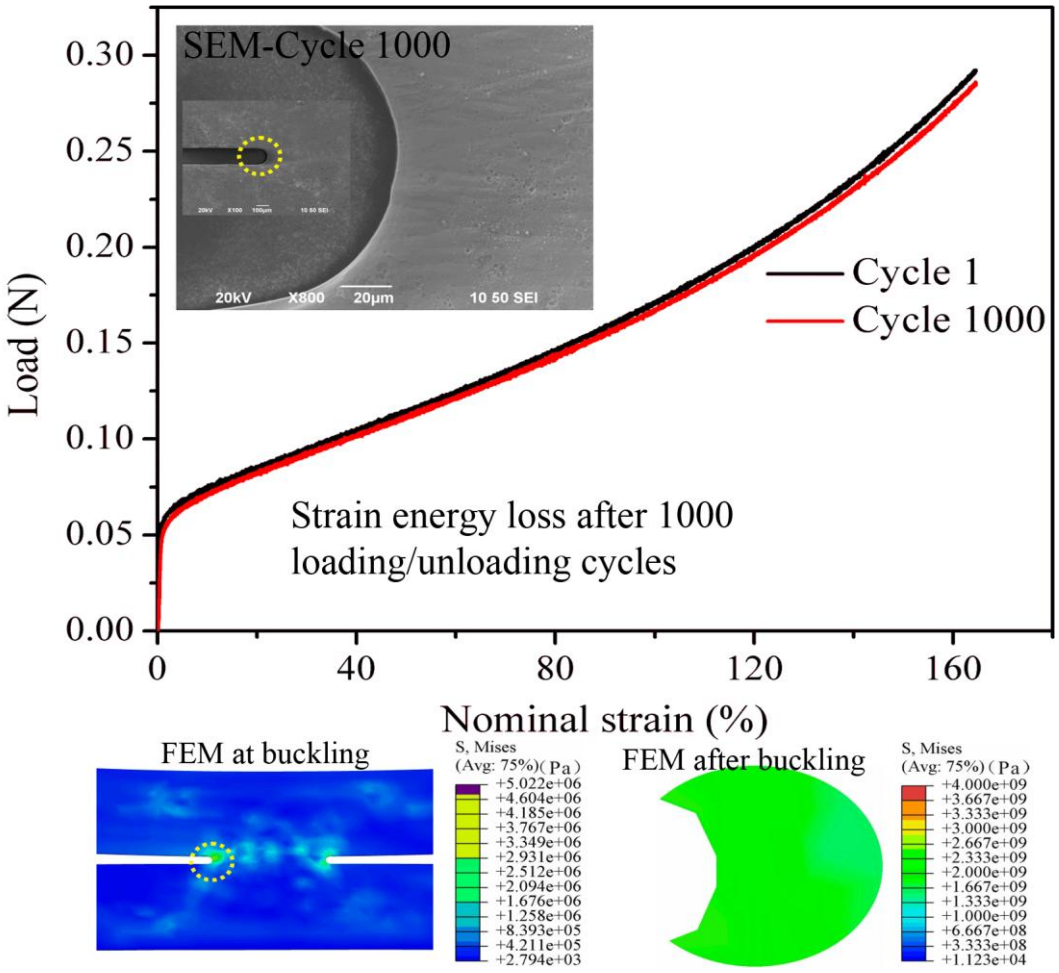

S. H. Chen *et al*.

Graphical abstract